THE ASTROPHYSICAL JOURNAL, 465:L57–L60, 1996 July 1


# OH IN THE LINE OF SIGHT TO HD 27778 AND $\zeta$ PERSEI

P. FELENBOK[1] AND E. ROUEFF[1, 2]
Departement d'Astrophysique Extragalactique et de Cosmologie and Unité de Recherche Associée 0173 du Centre National de la Recherche Scientifique, Observatoire de Paris-Meudon, Place Janssen, F 92195 Meudon Cedex, France
*Received 1996 February 20; accepted 1996 April 16*

## ABSTRACT

We present ground-based observations with the coudé spectrograph of the Canada-France-Hawaii Telescope aimed at revealing the presence of OH in the cloud located in front of HD 27778. The 3070–3080 Å spectral range was successfully studied and exhibited the presence of five transitions of OH located around 3072.0, 3078.4, and 3081.7 Å toward $\zeta$ Per and HD 27778. The deduced column density of OH in $\zeta$ Per confirms the previous results of Chaffee & Lutz and is equal to $10^{14}$ $cm^{-2}$ in HD 27778. An inversion in the populations of the $\Lambda$ doublet ground level is found in this line of sight. We also detected lines at 3072.9 Å which we tentatively identify as due to the presence of Ti II in two different atomic clouds, as was already found by Stokes toward $\zeta$ Per with a somewhat lower column density.

*Subject headings:* ISM: abundances — ISM: molecules — line: identification — stars: individual (HD 27778, $\zeta$ Per)

## 1. INTRODUCTION

Among stars with moderate extinction, the line of sight towards HD 27778 is one of the best studied. The brightness of the background star, $V = 6.36$ and $U = 6.18$, enables investigations of the absorbing medium both in the UV and visible spectral range. Joseph et al. (1986) report the gaseous abundance of 15 elements from *International Ultraviolet Explorer* (*IUE*) observations toward this direction and conclude that the observed strong depletion might be the best observational evidence of accretion onto dust. Moreover, this line of sight has a high abundance of molecules, including CO, CN, CH, $CH^+$, and NH. This latter molecule has indeed been recently detected (Meyer & Roth 1991) at 3358 Å in the diffuse clouds towards $\zeta$ Per and HD 27778. Such observations are also interesting in light of the fact that both $\zeta$ Per and HD 27778 have larger than normal far-UV extinction, presumably indicative of an overabundance of small grains in their line of sight. One might thus expect that grain catalysis reactions could lead to the production of NH as well as other molecules such as OH, as has been shown by Wagenblast et al. (1993) in the context of $\zeta$ Per. Since OH was not observed towards HD 27778, we have undertaken to detect this molecule in absorption in the $A$–$X$ (0–0) transition band at ≈3080 Å in order to complement the set of molecular data available in HD 27778. Indeed, the latest generation of CCD detectors has recently greatly improved the detection limits of weak absorption lines and programs to conduct deep searches down to ≈3050 Å spectral region become feasible in observatories at sufficiently high elevation such as the Canada-France-Hawaii Telescope (CFHT).

In this Letter, we report the discovery of interstellar OH towards HD 27778 and confirm its detection towards $\zeta$ Per from the three main absorption features at 3072, 3078, and 3081 Å. Spectral features around 3072.9 Å are also observed in both lines of sight and are tentatively identified as due to a Ti II resonance line belonging to an atomic cloud located in the vicinity of the molecular gas.

[1] Guest observers at the Canada-France-Hawaii telescope.
[2] roueff@obspm.fr.

## 2. OBSERVATIONS

Our team has, for a long time, had access to the CFH Telescope which is equipped with a UV coudé train. Its implementation on a high elevation site made it very attractive for interstellar absorption line observations down to the atmospheric cut off. Following the discovery of OH by Chaffee & Lutz (1977) in the direction of $\zeta$ Per, we made an attempt to confirm their observation at CFHT with the original f/8 Coudé spectrograph and a linear Reticon detector. Similar results were obtained, but no significant improvement was achieved, due to a relatively low spectral resolution and the high readout noise of the detector (Felenbok, Czarny, & Baudrand 1984). The recent commissioning of a new f/4 coudé spectrograph, GECKO, with a nominal spectral resolution of 120,000 and of the CFHT Orbit 464-24 CCD with a quantum efficiency above 0.7 at 3100 Å, allows us to reinvestigate the wavelength range below 3100 much more efficiently. This spectrograph is fitted with a 316 gr $mm^{-1}$ echelle grating and carries a Richardson image slicer coated for the UV. The spectrum is cross dispersed by a grism, and only two orders are falling on 200 pixels of the detector height. In the present case, orders 17 and 18 are recorded, and OH is seen in the later one. We decided then to make a new attempt to detect OH at 3080 and 3078 Å on the $\zeta$ Per line of sight and also to search for it toward a cloud of larger extinction with a much fainter background star, HD 27778. We were granted two nights, 1995 October 12 and 13. The first night was partially cirrus covered and the second one, clear. We made 3 exposures on $\zeta$ Per equivalent to 2 hr of integration time and 12 exposures on HD 27778 equivalent to a 9 hr integration time. We observed $\gamma$ Cas as comparison star. Figure 1 shows the spectra observed towards the three lines of sight, $\zeta$ Per, HD 27778, and $\gamma$ Cas in the 3072–3082 Å wavelength range. The identification of the absorption lines, which are obviously missing in the comparison $\gamma$ Cas star spectrum, is indicated on the $\zeta$ Per and HD 27778 spectra (see § 3).

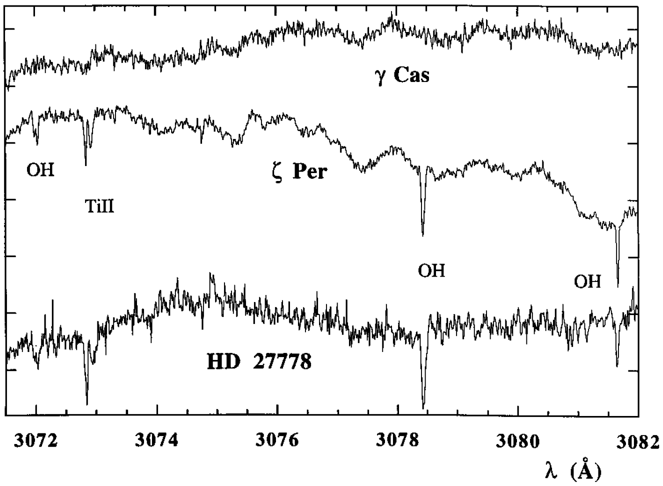


FIG. 1.—Comparison of $\gamma$ Cas, $\zeta$ Per, and HD 27778 in the 3070–3080 Å spectral region. All three spectra are displayed at the same relative intensity scale on the $y$-axis, with a vertical offset applied to $\zeta$ Per and HD 27778. Any interval between two subsequent ticks on the figure represents 5% of the normalized continuum. For the sake of comparison, all of the spectra are aligned in geocentric wavelengths. The labels OH and Ti II refer to the identification of the interstellar absorption features discussed in the text.

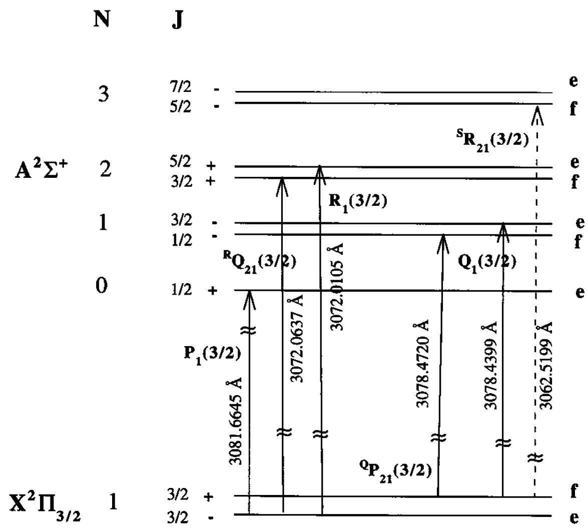


FIG. 2.—Level diagram of OH $A\ ^2\Sigma^+$–$X\ ^2\Pi_i$ (0, 0) showing the observed absorption transitions. The ground state $^2\Pi_i$ $J = 3/2$ is split by $\Lambda$ doubling into two levels of different parity $-(e)$ and $+(f)$. Each parity level is further separated in two hyperfine levels which are not resolved in the spectrum. All the electric dipole-permitted transitions from the $J = 3/2$ level of $X\ ^2\Pi_i$ are shown and have been observed in the present work, excepting the $^SR_{21}(3/2)$ satellite line at 3062.5199 Å displayed with a dashed arrow. The corresponding rest wavelengths in air are listed on the diagram.

## 3. DATA REDUCTION AND ANALYSIS

For data reduction, we recorded flat fields and bias in the usual way and used a Th-Ar wavelength calibration lamp. Thorium wavelengths were taken from Zalubas (1960) and cross checked with the Los Alamos Atlas (Palmer & Engleman 1983). The level of diffused light, measured in the interorder spacing, is around 10% and is removed from the stellar spectrum. The data were reduced with the IRAF software on a Sun workstation. The spectral resolution, measured as the FWHM of a Gaussian fit to a spectral line, is 30 mÅ on a comparison line and 34 mÅ on the OH 3081.7 Å line on the $\zeta$ Per summed spectrum, with a sampling of 0.011 Å pixel$^{-1}$. The S/N measured in the continuum at 3080 Å is around 600 for $\zeta$ Per and 120 for HD 27778. The measured wavelengths of the absorption lines are given in Table 1, and the features at 3081.6, 3078.4, and 3072.0 Å are unambiguously identified as due to the quoted OH $A$–$X$ band transitions. They show indeed a fairly constant shift between the observed and true values which are taken from Stark, Brault, & Abrams (1994). The least reliable values come from the $Q_1(3/2)$ and $^QP_{21}(3/2)$ lines around 3078.4 Å which are blended. Figure 2 displays the transitions pattern of the detected lines, from which we see that the $P_1$, $R_1$, and $^RQ_{21}$ lines arise from the lower $-(e)$ $\Lambda$ doublet component whereas the $Q_1$ and $^QP_{21}$ lines come from the upper $+(f)$ $\Lambda$ doublet component with the notations of Brown et al. (1975). The $R_1(3/2)$ and $^RQ_{21}(3/2)$ OH transitions at 3072 Å are observed for the first time in an

TABLE 1

SUMMARY OF THE WAVELENGTH MEASUREMENTS IN THE 3070–3090 Å RANGE

| | $\zeta$ PER | | HD 27778 | |
|---|---|---|---|---|
| REST WAVELENGTH (air) | Observed Wavelength (Å) | $\Delta\lambda$ | Observed Wavelength (Å) | $\Delta\lambda$ |
| OH: ........................ | | | | |
| $P_1(3/2)$: 3081.6645 ...... | 3081.616 ± 0.004 | −0.049 | 3081.606 ± 0.007 | −0.059 |
| $^QP_{21}(3/2)$: 3078.4720.... | 3078.420 ± 0.004 | −0.048 | 3078.427 ± 0.01 | −0.041 |
| $Q_1(3/2)$: 3078.4399...... | 3078.388 ± 0.007 | −0.052 | 3078.385 ± 0.007 | −0.055 |
| $^RQ_{21}(3/2)$: 3072.0637.... | 3072.014 ± 0.004 | −0.049 | 3072.008 ± 0.007 | −0.055 |
| $R_1(3/2)$: 3072.0105 ...... | 3071.960 ± 0.004 | −0.049 | 3071.951 ± 0.007 | −0.058 |
| Ti II: 3072.9706............. | 3072.812 ± 0.004[a] | 4.95* | 3072.811 ± 0.007[c] | 4.25* |
| | 3072.901 ± 0.004[b] | 13.6* | 3072.92 ± 0.01[d] | 15.0* |

NOTE.—$\Delta\lambda$ is the wavelength shift between the observed and rest wavelength in Å. The mean wavelength shift from OH measurements is (0.049 ± 0.005) Å for $\zeta$ Per and (0.057 ± 0.007) Å for HD 27778. The data from the 3078 Å lines, which are blended, were given a lower weight. Heliocentric velocities (in km s$^{-1}$) of 15.7 ± 0.5 and 14.3 ± 0.7 are then deduced for the OH lines in $\zeta$ Per and HD 27778, respectively, which compare to 14.1 ± 1.1 and 15.6 ± 1.1 deduced for NH lines from Meyer & Roth (1991). Values marked with an asterisk denote heliocentric velocities in km s$^{-1}$.

[a] A component of Ti II lines observed toward $\zeta$ Per.
[b] A component of Ti II lines observed toward $\zeta$ Per.
[c] A component of Ti II lines observed toward HD 27778.
[d] A component of Ti II lines observed toward HD 27778.

TABLE 2

MOLECULAR PARAMETERS, EQUIVALENT WIDTHS, AND COLUMN DENSITIES OF THE ABSORBING LEVELS IN THE OH AND Ti II TRANSITIONS OBSERVED TOWARD $\zeta$ PERSEI AND HD 27778

| | REST WAVELENGTH $\lambda_{air}$ (Å) | | | | | |
|---|---|---|---|---|---|---|
| | 3081.6645 | 3078.4399 + 3078.4720 | 3072.0105 | 3072.0637 | 3072.9706 | |
| | OH (0–0) $A$–$X$ | | | | | |
| PARAMETER | $P_1(3/2)$ | $Q_1(3/2)$ + ${}^QP_{21}(3/2)$ | $R_1(3/2)$ | ${}^RQ_{21}(3/2)$ | Ti II $a\ {}^4F_{3/2}$–$z\ {}^4D^o_{1/2}$ | |
| $f$ value | 6.48 (−4) | 1.05 (−3) | 1.8 (−4) | 2.7 (−4) | 0.109 | 0.109 |
| $\zeta$ Per: $W_\lambda$ (mÅ) | 1.11 ± 0.05 | 1.67 ± 0.08 | 0.37 ± 0.05 | 0.52 ± 0.05 | 1.5 ± 0.1[a] | 1.6 ± 0.1[a] |
| $\zeta$ Per: $N$ (cm$^{-2}$) | [2.0 ± 0.1] (13) | [1.9 ± 0.1] (13) | [2.5 ± 0.3] (13) | [2.3 ± 0.2] (13) | [1.6 ± 0.1] (11) | [1.8 ± 0.1] (11) |
| HD 27778: $W_\lambda$ (mÅ) | 2.2 ± 0.1 | 5.3 ± 0.15 | 0.53 ± 0.1 | 1.0 ± 0.1 | 3.2 ± 0.1[b] | 2.8 ± 0.2[b] |
| HD 27778: $N$ (cm$^{-2}$) | [4.0 ± 0.2] (13) | [6.0 ± 0.2] (13) | [3.5 ± 0.7] (13) | [4.3 ± 0.4] (13) | [3.5 ± 0.1] (11) | [3.1 ± 0.2] (11) |

NOTE.—Values in parenthesis refer to powers of ten. The oscillator strength of the Ti II line is taken from Morton 1991.
[a] Two different components of ionized gas observed toward $\zeta$ Per.
[b] Two different components of ionized gas observed toward HD 27778.

interstellar spectrum.[3] The values of the heliocentric velocities deduced from the observations are also given in Table 1 and agree reasonably well with the values reported by Meyer & Roth (1991) for the molecular clouds in $\zeta$ Per and HD 27778. We also observe two lines around 3072.9 Å towards $\zeta$ Per which are very close to the rest wavelength of the $a\ {}^4F_{3/2}$–$z\ {}^4D^o_{1/2}$ transition of Ti II at 3072.9706 Å as has been recently redetermined by Fourier transform spectroscopy (Johansson & Zapadlik 1996 private communication). Ti II has indeed been observed towards $\zeta$ Per by several observers (Chaffee 1974; Stokes 1978; Hobbs 1979; Magnani & Salzer 1991) via another resonance line at 3383.7 Å. We then identify the features at 3072.9 Å as Ti II belonging to different cloud components from that where OH is observed, for which heliocentric velocities are also displayed in Table 1, and which are within the range of velocities given by Stokes (1978). In the same way, we also attribute the remaining feature at 3072.9 Å observed in HD 27778 to Ti II but, to our knowledge, no other measurements of Ti II are reported towards HD 27778. Moreover, we have access to the 3250–3272 Å range in the 17th order of the grating; yet, no spectral feature was observed in this spectral range.

The equivalent widths listed in Table 2 for the interstellar OH and Ti II lines towards $\zeta$ Per and HD 27778 were measured from Gaussian fits to the line profiles. When the lines were not satisfactorily resolved, which is the case for the 3078 Å lines for HD 27778, we measured the total area of the combined lines. We checked this approach on the 3078 Å lines on $\zeta$ Per for which both treatments are possible, and the difference in the equivalent widths from the two methods is below 0.05 mÅ. The errors in the equivalent widths arise from two major sources: the placement of the continuum, and the statistical error due to the noise in the spectrum. The statistical error $\sigma_s$ in the measured equivalent width is given by Jenkins et al. (1973):

$$\sigma_s = (\Delta\lambda\sqrt{n})/(\mathrm{S/N}),$$

where $n$ is the number of pixels over the line profile, $\Delta\lambda$ is the spectral dispersion (Å pixel$^{-1}$), and S/N is the signal to noise ratio pixel$^{-1}$, measured in the continuum near the absorption lines. We derive the rms error on $W_\lambda$ by checking the constancy of the quantity $W_\lambda/(f\lambda^2)$, which is proportional to the column density of the absorbing level, for the concerned lines (3081 and 3072 Å). The equivalent widths of the lines at 3078 and 3081 Å are consistent with the values determined by Chaffee & Lutz (1977) for $\zeta$ Per. The oscillator strengths listed are somewhat different from those reported previously due to a normalization error in the rotational strengths factors which has been corrected in Roueff (1996).

[3] These lines have also been observed in Perseus OB2 (Federman, Weber, & Lambert 1996), according to the referee, J. Black.

## 4. DISCUSSION AND PERSPECTIVES

### 4.1. OH

As shown in Roueff (1996), the determination of the total column density of OH requires inclusion of both the $e$ and $f$ absorbing level of the ground rotational state $J = 3/2$ (the hyperfine splitting is not resolved). If the lines are optically thin, we may calculate the column density of each absorbing level from the following formula:

$$N = 1.13\ 10^{20}\, W_\lambda/(f\lambda^2),$$

where $\lambda$ and $W_\lambda$ are in Å and $N$ in cm$^{-2}$. The resulting column densities are given in Table 2. We recall that the transitions at 3081 and 3072 Å sample the same absorbing ground level ($e$) whereas the 3078 Å lines come from the excited ($f$) level of the $\Lambda$ doublet in the ground $X\ {}^2\Pi_i$ electronic state. The determinations of the column densities of the absorbing levels from the different measurements are consistent. However, we do not include the value deduced from the least accurate 3072.0105 Å line in the averaging, and we derive $N(e) = [2.15 \pm 0.15] \times 10^{13}$ cm$^{-2}$ and $N(f) = [1.9 \pm 0.1] \times 10^{13}$ cm$^{-2}$ for $\zeta$ Per, and $N(e) = [4.15 \pm 0.3] \times 10^{13}$ cm$^{-2}$ and $N(f) = [6.0 \pm 0.2] \times 10^{13}$ cm$^{-2}$ for HD 27778. The energy splitting $\Delta E$ is 0.080 K, corresponding to a frequency of 1666.625 MHz. Our measurements yield values of the excitation temperature defined by: $T_{exc} = \Delta E(\mathrm{K})/\ln[N(e)/N(f)]$, equal to (0.65 ± 0.6) K for $\zeta$ Per, and −0.22 ± 0.06 K for HD 27778, much lower than the expected kinetic temperature. The real physical significance of these excitation temperatures remains to be understood. The negative value of the excitation temperature in HD 27778 reveals the presence of a level inversion mechanism which comes probably from the dust infrared radiation. Table 3 gives the column densities of the observed molecules towards both directions. The results show an increase of the molecular column density of OH in HD 27778 compared to $\zeta$ Per, which follows the trends observed for NH, CN, and $CH^+$. An

TABLE 3

SUMMARY OF THE OBSERVED MOLECULAR COLUMN DENSITIES TOWARDS THE TWO LINES OF SIGHT

| Species | $\zeta$ Per Observed $N$ ($cm^{-2}$) | HD 27778 Observed $N$ ($cm^{-2}$) |
|---|---|---|
| OH.......... | [4.05 ± 0.4] (13)[a] | [10.2 ± 0.4] (13)[a] |
| NH.......... | 9.0 (11)[b] | 2.7 (12)[b] |
| CH.......... | 2.0 (13)[c] | 2.9 (13)[d] |
| $CH^+$ ......... | 3.5 (12)[e] | 7.0 (12)[f] |
| CN.......... | 3.0 (12)[g] | 1.5 (13)[f, d] |
| $C_2$.......... | 1.9 (13)[h] | 3.8 (13)[d] |
| CO.......... | 5.4 (14)[i] | 6.6 (15)[j] |
| $H_2$ .......... | 4.8 ± 1.0 (20)[k] | 1.1 ± 0.3 (21)[l] |

[a] From the analysis of present observations.
[b] Meyer & Roth 1991.
[c] Jura & Meyer 1985.
[d] Federman et al. 1994.
[e] Federman 1982.
[f] Reported in Meyer & Roth 1991.
[g] Meyer & Jura 1985.
[h] Danks & Lambert 1983, reanalyzed by van Dishoeck & Black 1989.
[i] Snow 1977 (with updated $f$-values from van Dishoeck & Black 1986).
[j] Joseph et al. 1986.
[k] Savage et al. 1977.
[l] Reported in Joseph et al. 1986.

important question is the respective role between gas phase and surface chemistry. Indeed, as stressed by Crutcher & Watson (1976) and Mann & Williams (1984), NH is almost exclusively formed via surface processes whereas OH can result both from grain and gas chemistry (Wagenblast et al. 1993). However, such quiescent chemistry is not able to explain the observed abundance of $CH^+$ which requires some "hot" chemistry which may be provided by shocks (Pineau des Forêts et al. 1986) or by turbulence (Falgarone, Pineau des Forêts, & Roueff 1995; Spaans, Black, & van Dishoeck 1996). But, this hot chemistry is also a source of OH mainly via the reaction

$$O + H_2 \rightarrow H + OH,$$

which has an activation barrier of about 3000 K, and all these different possibilities should be included in realistic models. This is beyond the scope of the present paper but we intend to investigate such models by combining gas phase and grain surface reactions.

### 4.2. *Ti II*

The total column density of Ti II is found to be equal to $[3.4 \pm 0.2] \times 10^{11}$ $cm^{-2}$ and $[6.6 \pm 0.3] \times 10^{11}$ $cm^{-2}$ in front of $\zeta$ Per and HD 27778, respectively. The value towards $\zeta$ Per is larger by about a factor of 2 than the value mentioned by Stokes (1978) or Magnani & Salzer (1991) who observed the transition at 3384 Å, arising from the same lower level. The origin of the discrepancy is not clear, but we should stress that our observations should not be affected by opacity problems as is the case for 3384 Å which has an oscillator strength more than three times larger than the present line. The study of the depletion of Ti in the lines of sight considered would also require the determination of the column density of the neutral species which has several transitions which may be observed from the ground (Morton 1991). This program will be undertaken in future studies.

P. F. is grateful to V. Cayatte for introducing him to the IRAF labyrinth and to P. Jablonka and D. Proust for valuable advice for a safe navigation between the different packages of this data reduction software. We gratefully thank Drs. Johansson and Zapadlik for supplying their new unpublished values of the wavelengths of Ti II. We are also indebted to the referee, J. Black, for relevant comments and for pointing out the wavelength tables for Th/Ar spectrum and OH lines.

REFERENCES

Brown, J. M., et al. 1975, J. Mol. Spectrosc., 55, 500
Chaffee, F. H., Jr. 1974, ApJ, 189, 427
Chaffee, F. H., Jr., & Lutz, B. 1977, ApJ, 213, 394
Cheung, A. S.-C., Chan, C. M.-T., & Sze, N. S.-K. 1995, J. Mol. Spectrosc., 174, 205
Crutcher, R. M., & Watson, W. D. 1976, ApJ, 209, 778
Danks, A. C., & Lambert, D. L. 1983, A&A, 124, 188
Falgarone, E., Pineau des Forêts, G., & Roueff, E. 1995, A&A, 300, 870
Federman, S. R. 1982, ApJ, 257, 125
Federman, S. R., Strom, C. J., Lambert, D. L., Cardelli, J. A., Smith, V. V., & Joseph, C. L. 1994, ApJ, 424, 772
Federman, S. R., Weber, J., & Lambert, D. L. 1996, ApJ, in press
Felenbok, P., Czarny, J., & Baudrand, J. 1984, Canada-France-Hawaii Telescope Bulletin no. 10, 9
Hobbs, L. M. 1979, ApJ, 229, L129
Jenkins, E. B., et al. 1973, ApJ, 181, L122
Joseph, C. L., Snow, T. P., Jr, Seab, C. G., & Crutcher, R. M. 1986, ApJ, 309, 771
Jura, M., & Meyer, D. M. 1985, ApJ, 294, 238
Magnani, L., & Salzer, J. J. 1991, AJ, 101, 1429
Mann, A. P. C., & Williams, D. A. 1984, MNRAS, 209, 33
Meyer, D. M., & Jura, M. 1985, ApJ, 297, 119
Meyer, D. M., & Roth, K. C. 1991, ApJ, 413, L67
Morton, D. C. 1991, ApJS, 77, 119
Palmer, B. A., & Engleman, R., Jr. 1983, Los Alamos Atlas (Los Alamos: LANL)
Pineau des Forêts, G., Flower, D. R., Hartquist, T. W., & Dalgarno, A. 1986, MNRAS, 220, 801
Roueff, E. 1996, MNRAS, 279, L37
Savage, B. D., Bohlin, R. C., Drake, J. F., & Budich, W. 1977, ApJ, 216, 391
Snow, T. P. 1977, ApJ, 216, 724
Spaans, M., Black, J. H., & van Dishoeck, E. F. 1996, ApJ, in press
Stark, G., Brault, J. W., & Abrams, M. C. 1994, J. Opt. Soc. Am. B, 11, 3
Stokes, G. M. 1978, ApJS, 36, 115
van Dishoeck, E. F., & Black, J. H. 1986, ApJS, 62, 109
———. 1989, ApJ, 340, 273
Wagenblast, R., Williams, D. A., Millar, T. J., & Nejad, L. A. M. 1993, MNRAS, 260, 420
Zalubas, R. 1960, NBS Monogr. 17, USA